PHYSICALLY-BASED SYNTHESIS OF NONLINEAR CIRCULAR MEMBRANES

Riccardo Marogna
Dept. of Information Engineering
University of Padova
Padova, Italy
marognar@dei.unipd.it

Federico Avanzini
Dept. of Information Engineering
University of Padova
Padova, Italy
avanzini@dei.unipd.it

ABSTRACT

This paper investigates the properties of a recently proposed physical model of nonlinear tension modulation effects in a struck circular membrane. The model simulates dynamic variations of tension (and consequently of partial frequencies) due to membrane stretching during oscillation, and is based on a more general theory of geometric nonlinearities in elastic plates. The ability of the nonlinear membrane model to simulate real-world acoustic phenomena is assessed here through resynthesis of recorded membrane (rototom) sounds. The effects of air loading and tension modulation in the recorded sounds are analyzed, and model parameters for resynthesis are consequently estimated. The example reported in the paper show that the model is able to accurately simulate the analyzed rototom sounds.

1. INTRODUCTION

With respect to other classes of instruments (e.g.string or wind instruments) drums are relatively less studied in the literature of physical modeling (see e.g. the two tutorial papers [1, 2]). Membrane models proposed in previous works are mainly based on 2-D or 3-D digital waveguide meshes (DWM [3]), which can provide accurate simulation of wave propagation medium terms, depending on the mesh topology [4], and with additional processing to compensate for dispersion [5]. Finite-difference schemes have also been used (see [6] for an analysis of various schemes). Models based on modal synthesis [7] have been introduced. Cook [8] proposed a series of "physically-informed" approaches to the modeling of percussion sounds, including modal synthesis. Rabenstein and coworkers have applied the functional transformation method to the simulation of rectangular and circular linear membranes [9].

The latter authors have proposed a nonlinear extension of their approach to simulate tension modulation effects in a rectangular membrane [10]. Tension modulation in strings and membranes occurs because in the large oscillation regime the assumption of constant string length (or membrane area) does not hold, and the tension varies in dependence of the instantaneous displacement. As a consequence, the oscillation frequency at large displacements is increased, and the resulting sound exhibits characteristic glides.

Models for tension modulation in strings have been discussed in the context of both waveguide [11] and modal [12, 13] approaches. An extension to the 2-D case of rectangular membranes has been proposed in [10]. However, there appear to be no previous analysis of physical models for sound synthesis of tension-modulated circular membranes, although the circular geometry is more relevant than the rectangular one for musical applications.

More general models of geometrical nonlinearities in membranes can be borrowed from the theory of vibrations of elastic plates [14]. We have recently proposed such a model in [15] for a 2-D problem with circular geometry, and have shown that it can be efficiently integrated into a modal synthesis engine.

The main goal of this paper is to assess the effectiveness of the model in reproducing tension modulation effects observed in real membranes. To this end, a set of recordings from three rototoms was collected. The rototom has been chosen as a test instrument because *by construction* it approaches quite closely the ideal case of a single circular membrane with fixed boundaries, with no other mechanisms affecting appreciably sound production (shell, air cavity, coupling with a second membrane).

The recorded sounds have been analyzed in order to extract the most relevant parameters, particularly with regard to the effects or air loading (detuning and increased dissipation of lower partials), and those of tension modulation (initial glides of partials). Resynthesis has then been obtained by fitting the geometrical and physical parameters of the model to those of the recorded membranes. The results show that the model provides convincing simulation of the most salient sound features.

Section 2 summarizes the physical model recently proposed in [15] for tension modulation in a circular membrane, and discusses a numerical realization. Section 3 discusses the main findings from analysis of the sounds recorded from real membranes, and presents results obtained from the resynthesis of the membrane sounds with the proposed physical model.

Table 1: *Physical and geometrical membrane parameters.*

Symbol	Unit	Meaning
σ	Kg/m^2	Surface density
T_0	N/m	Surface tension
d_1	Kg/sm^2	Freq. independent dissipation coefficient
d_3	Kg/sm	Freq. dependent dissipation coefficient
E	N/m^2	Young modulus
υ	—	Poisson ratio
R	m	Radius

2. A MODEL FOR TENSION MODULATION IN A CIRCULAR MEMBRANE

2.1. Linear circular membrane

This section summarizes briefly the modal description of a linear circular membrane with dispersion and dissipation (an equivalent formulation can be found in [9]). The vertical displacement $z(r,\varphi,t)$ of the membrane, driven by a force density $f^{(\text{ext})}(r,\varphi,t)$, is governed by the following equation [16]:

$$D\nabla^4 z(r,\varphi,t) + \sigma\frac{\partial^2 z(r,\varphi,t)}{\partial t^2} - T_0\nabla^2 z(r,\varphi,t) + d_1\frac{\partial z(r,\varphi,t)}{\partial t} + d_3\frac{\partial \nabla^2 z(r,\varphi,t)}{\partial t} = f^{(\text{ext})}(r,\varphi,t), \quad (1)$$

where the coefficient $D = Eh^3/12(1-\upsilon^2)$ is the bending stiffness of the membrane. The units and meanings of all the physical parameters in Eq. (1) are listed in Table 1. Ideal boundary conditions are represented by zero deflection and skewness at the boundary $\mathcal{B} = \{(r,\varphi) \,:\, r = R\}$, i.e.

$$z(r,\varphi,t)\big|_{(r,\varphi)\in\mathcal{B}} = 0, \quad \nabla^2 z(r,\varphi,t)\big|_{(r,\varphi)\in\mathcal{B}} = 0, \quad (2)$$

Given these boundary conditions together with suitable initial conditions (e.g. zero initial displacement and zero initial velocity), Eq. (1) has a unique solution. The general solution can be expressed in terms of its normal modes, i.e. particular solutions of type $\bar{z}(t)K(r,\varphi)$. With the boundary conditions considered here, the equation has a numerable set of modes with spatial eigenfunctions [17]

$$K_{n,m}(r,\varphi) = \cos[n(\varphi-\varphi_0)]J_n\left(\mu_{n,m}\frac{r}{R}\right), \quad (3)$$

where $n \geq 0$, $m \geq 1$, and $\mu_{n,m}$ is the m-th zero of the n-th order Bessel function of the first kind, J_n. These spatial eigenfunctions define a Sturm-Liouville (SL) transform [9]). The SL transform $\bar{g}$ of a function g and the inverse SL transform of $\bar{g}$ are

$$\begin{aligned} \bar{g}_{n,m}(t) &= \int_0^{2\pi}\int_0^R g(r,\varphi,t)K_{n,m}(r,\varphi)\, r dr d\varphi, \\ g(r,\varphi,t) &= \sum_{n=0}^{+\infty}\sum_{m=1}^{+\infty}\frac{\bar{g}_{n,m}(t)K_{n,m}(r,\varphi)}{\| K_{n,m}(r,\varphi)\|_2^2}. \end{aligned} \quad (4)$$

By virtue of these transformations, one can see that the original PDE (1) for z is turned into a set of ordinary differential equations for the modes $\bar{z}_{n,m}$:

$$\ddot{\bar{z}}_{n,m}(t) + \frac{1}{\sigma}\left[d_1 + d_3\left(\frac{\mu_{n,m}}{R}\right)^2\right]\dot{\bar{z}}_{n,m}(t) + \left(\frac{\mu_{n,m}}{R}\right)^2\left[\frac{D}{\sigma}\left(\frac{\mu_{n,m}}{R}\right)^2 + \frac{T_0}{\sigma}\right]\bar{z}_{n,m}(t) = \frac{\bar{f}^{(\text{ext})}_{n,m}(t)}{\sigma}, \quad (5)$$

where the forcing term $\bar{f}^{(\text{ext})}_{n,m}$ is the SL transform of $f^{(\text{ext})}$. Therefore the mode $\bar{z}_{n,m}$ is a forced second order oscillator whose parameters are determined by those of the original PDE.

2.2. Nonlinear terms: impact force, tension modulation

In the following we summarize the nonlinear membrane model proposed in [15]. We assume that the membrane is driven by an impact force ideally applied at a hit point $x_h = (r_h, \varphi_h)$ of the membrane surface. In this assumption the force density is $f^{(\text{ext})}(x,t) = F_h(t)\delta(x - x_h)$ (where $x = (r,\varphi)$ and δ is a 2D Dirac Delta). Then $\bar{f}^{(\text{ext})}_{n,m}$ takes the form

$$\bar{f}^{(\text{ext})}_{n,m}(t) = F_h(t)K_{n,m}(r_h,\varphi_h). \quad (6)$$

The force F_h is estimated with an impact model originally proposed in [18], and previously applied to the synthesis of impact sounds [19]. If the hammer is a point mass m_h moving with a trajectory $z_h(t)$ and hitting the membrane at x_h, then F_h is a function of the compression $\zeta(t) = z(r_h,\varphi_h,t) - z_h(t)$:

$$F_h(\zeta(t),\dot{\zeta}(t)) = k\zeta(t)^\alpha + \lambda\zeta(t)^\alpha\dot{\zeta}(t), \quad \zeta > 0, \quad (7)$$

while $F_h = 0$ otherwise. The impact model parameters are the force stiffness k, the force dissipation coefficient λ, and the exponent α (which depends on the local geometry around the contact area). The hammer dynamics is completely determined by the equation $m_h\ddot{z}_h = F_h$.

Another very important nonlinear effect encountered in real membranes is tension modulation. Since the membrane area varies during oscillation, the tension also varies in dependence of the membrane displacement, causing variations of the frequency content during the sound evolution. In [15] we have presented a model for tension modulation, in the assumption of homogeneous and isotropic membrane material, and of uniform clamping.

The model is derived from the general theory of elastic plates. Specifically, it is based on the so-called Berger approximation of the von Karman equations, which describe the dynamics of thin plates subjected to lateral and in-plane forces [14]. Such an approximation has the fundamental advantage of decoupling the von Karman equations for stress

and displacement, resulting in a single fourth-order PDE which can be written as follows:

$$D\nabla^4 z + \sigma\frac{\partial^2 z}{\partial t^2} - [T_0 + T_{NL}(z)]\nabla^2 z + \\ + d_1\frac{\partial z}{\partial t} + d_3\frac{\partial \nabla^2 z}{\partial t} = f^{(\text{ext})}, \quad (8)$$

where, for the specific case of the membrane, the nonlinear function $T_{NL}(z)$ can be interpreted as the surface tension generated in dependence of the displacement z, in addition to the tension at rest T_0. Such function has the form [14]

$$T_{NL}(z) = \frac{Eh}{2\pi R^2(1-\upsilon^2)} \cdot \\ \int_0^R\int_0^{2\pi}\left[\left(\frac{\partial z}{\partial r}\right)^2 + \frac{1}{r^2}\left(\frac{\partial z}{\partial \varphi}\right)^2\right] r d\varphi dr. \quad (9)$$

The double integral in Eq. (9) can be interpreted as the difference between the membrane area $A(z)$ corresponding to the displacement z, and the area at rest $A_0 = \pi R^2$. Accordingly, the function $T_{NL}(z)$ can be interpreted as a spatially uniform tension modulation term, which depends only on the total area $A(z)$, in analogy with the Kirchhoff-Carrier equations for tension-modulated strings.

In the remainder of the paper we regard the nonlinear tension term as an excitation term $f^{(\text{tm})}(z) = T_{NL}(z)\nabla^2 z$, which acts on the right-hand side of Eq. (8) similarly to the impact force term $f^{(\text{ext})}$. Analogously, in the SL transformed domain we regard tension modulation as an additional forcing term $\bar{f}^{(\text{tm})}_{n,m}$ acting on the second order oscillator (5). Such term has the form

$$\bar{f}^{(\text{tm})}_{n,m}(\bar{z}) = -\left(\frac{\mu_{n,m}}{R}\right)^2 \bar{T}_{NL}(\bar{z})\bar{z}_{n,m}, \quad (10)$$

with

$$\bar{T}_{NL}(\bar{z}) = \frac{Eh}{4R^2(1-\upsilon^2)}\sum_{n,m}\frac{\mu^2_{n,m}\bar{z}^2_{n,m}}{\| K_{n,m}\|_2^4} J^2_{n+1}(\mu_{n,m}). \quad (11)$$

This equation is obtained by first applying the SL transform to $f^{(\text{tm})}$, and then by rewriting T_{NL} as a function of $\bar{z}$. Details about the derivation are reported in [15].

By looking at the second-order oscillators (5) and at the nonlinear forcing terms (10,11), one can see that the tension-modulated membrane model is written in terms of the modal variables $\bar{z}_{n,m}$ only.

2.3. A discrete-time model

The membrane model is realized as a bank of second order resonators, each of which represents one mode of oscillation. Specifically, in the Laplace domain the (n, m) normal

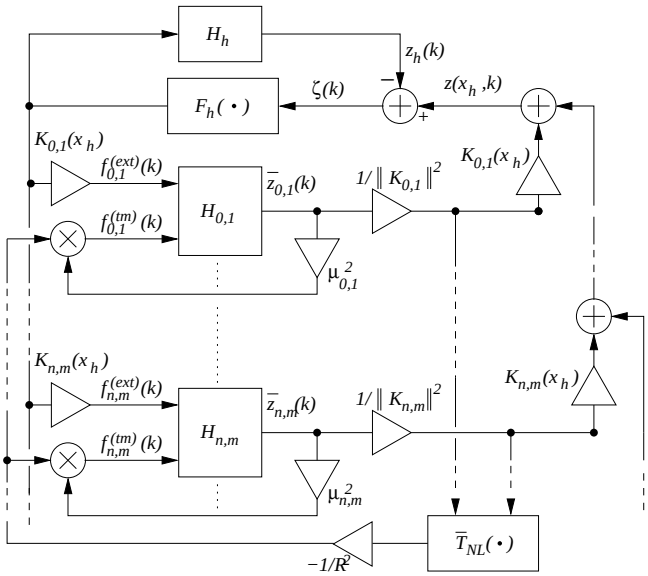

Figure 1: *Block scheme for the discrete-time realization of the nonlinear membrane model.*

mode is the output of the second order filter

$$H_{n,m}(s) = \frac{\sigma^{-1}}{s^2 + 2\alpha_{n,m}s + \omega^2_{n,m}}, \quad (12)$$

where the dependence of the loss factor $\alpha_{n,m}$ and the center frequency $\omega_{n,m}$ on the PDE parameters is determined from Eq. (5): the coefficient of $\dot{\bar{z}}_{n,m}$ equals $2\alpha_{n,m}$, and the coefficient of $\bar{z}_{n,m}$ equals $\omega^2_{n,m}$. Similarly, the hammer displacement z_h is the output of the second order filter $H_h(s)m_h/s^2$ applied to the impact force F_h. The filters $H_{n,m}$ and H_h are discretized using the bilinear transform. The resulting block scheme is shown in Fig. 1. The impact force of Eq. (7) is applied at the hit point x_h. The nonlinear tension modulation is computed according to Eq. (11) and can be applied to all the simulated modes or to a subset.

Note that the all the nonlinear terms appearing in the block scheme depend nonlinearly on instantaneous values of the modal displacements $\bar{z}_{n,m}$ and act as feedback to the filters $H_{n,m}$. Consequently, delay-free computational loops are generated, and a nonlinear implicit system must be solved at every computation step in order to find new values of all system variables. We have shown in [15] that the block scheme of Fig. 1 can be solved by applying a general technique for the computation of nonlinear digital filter networks with delay-free loops, recently proposed in [20].

The sound signal is taken to be the membrane displacement at a certain "pick-up" point x_p, which does not necessarily coincide with the hit point. Such displacement signal is obtained by applying the inverse SL transform, (the second equation in (4)) at the point x_p.

Figure 2: *Recording setup: the rototom is tuned with a precision drum tuner, and the support is damped with foam.*

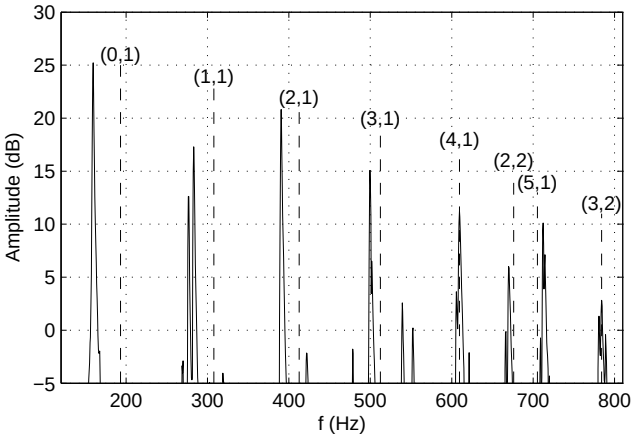

Figure 3: *First partials extracted from rototom sound spectrum. For each mode, the corresponding nodal pattern* (n, m) *is indicated.*

3. RESYNTHESIS OF REAL MEMBRANE SOUNDS

3.1. Recordings

The rototom is a drum instrument consisting of a single head in a die-cast metallic frame (often aluminium), without a shell. Rototoms are most typically used to extend the tom range of a standard drum kit, and their timbre is qualitatively similar to that of toms with the carry head removed. They can be tuned by rotating the head, which is inserted into a threaded metal ring: head rotation changes the tension hoop relative to the rim, and consequently the tension of the membrane.

Rototom sounds were recorded for subsequent analysis. The recording equipment included an AKG-C414 condenser microphone and an EDIROL UA-101 sound board. Sound were acquired using a sample rate $F_s = 96$ KHz, with a resolution of 24 bits. The recordings were not taken in anechoic settings and therefore include the impulse response of the medium-size room where they were acquired. Since the rototom frame was found to produce distinctive and persistent resonances when hitting the membrane, it was damped with foam in order to minimize this effect. A picture of the setup used for the recordings is shown in Fig. 2

Sounds were recorded with a wooden drumstick hitting the membrane at three different hit points (with normalized radius values $r/R = 0,\ 0.5,\ 0.8$). Two main impact strength levels ('soft' and 'strong') were used, although the impact velocity was not recorded. In order to properly tune the membrane to an uniform tension, a precision drum tuner was used (see Fig. 2). The tuner provides a measure (on an arbitrary scale) of the membrane tension along the surface. The tuning procedure is accomplished by moving the tuner along the membrane circumference, resulting in an approximately constant membrane tension along the whole surface. However, the tuner does not provide an absolute physical value of the surface tension.

3.2. Analysis

The recorded rototom sounds were analyzed for resynthesis purposes. Since some physical parameters (e.g. the membrane tension) could not be measured, they had to be estimated through *ad-hoc* analysis on the sound recordings. For the sake of clarity, all the analysis examples and related plots discussed in this section are based on the same recorded sound, obtained with a hit point at $r/R = 0.5$ and with a 'strong' impact level.

First, a matching procedure between theoretical modal frequencies and the measured ones has been performed, in order to identify the mode series of the membrane. An example is shown in Fig. 3. As expected, partial frequencies are lowered with respect to theoretical values, due to the air load acting on the membrane. This effect is noticeable mostly for frequencies below 500 Hz [17]. In fact from Fig. 3 one can notice that the error between measured and theoretical frequencies decreases with increasing frequency and becomes extremely small above 500 Hz.

In order to take into account this air loading effect, the simplified model reported in [17] was used (a similar model has been used in [21] in the context of waveguide membrane modeling). The model makes use of a piston-like approximation for which the effective air mass loading is given by:

$$m_{\text{air}} = \frac{8}{3}\rho_0 R^3, \qquad \text{for} \quad f < \frac{c}{4\pi R}, \tag{13}$$

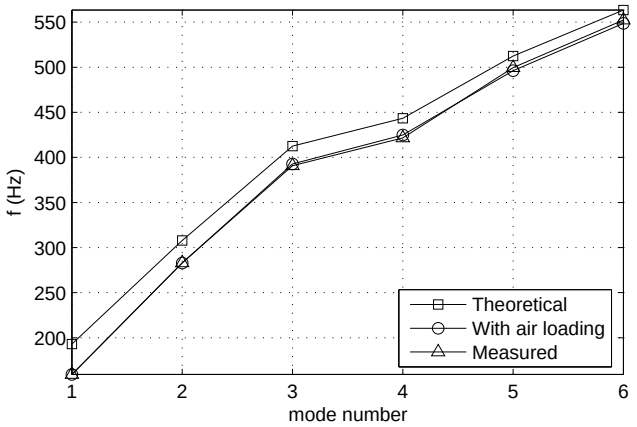

Figure 4: *Air load modeling through the piston-like approximation: comparison between theoretical, air-loaded, and measured frequencies.*

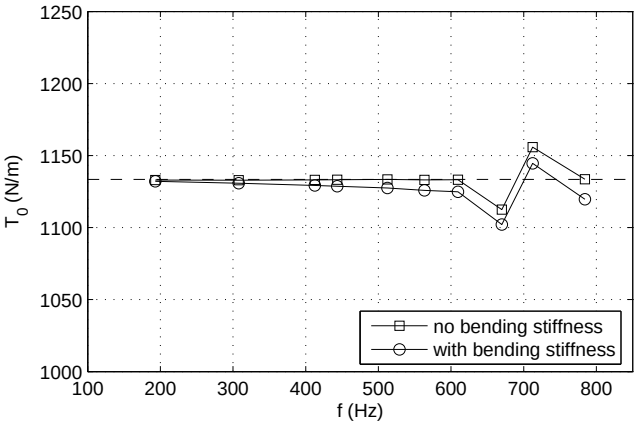

Figure 5: *Equivalent membrane tension estimated from measured frequencies (corrected with the air load model).*

and decreases for higher frequencies as $1/f^2$. The frequencies of the modes (n, m) affected by air mass loading are lowered to values $\omega_{n,m}^{(\text{air})}$, which are related to the theoretical values $\omega_{n,m}$ through the relation

$$\omega_{n,m}^{(\text{air})} = \omega_{n,m} \cdot \sqrt{\frac{\sigma}{\sigma + \sigma_{\text{air}}}}, \tag{14}$$

where $\sigma_{\text{air}} = m_{\text{air}}/\pi R^2$ is the resulting added surface density corresponding to the m_{air} added mass. Figure 4 shows an example of comparison between theoretical modal frequency values, those measured from the recording, and those estimated with the air-load correction by means of Eq. (14). It can be seen that the air load model matches extremely well the measured values. For higher mode numbers the theoretical curve progressively approaches the other two.

Having estimated a set of partial frequencies corrected according to the air load model, the corresponding membrane tension $T_{0_{n,m}}$ was estimated from Eq. (5) as:[1]

$$T_{0_{n,m}} = \sigma\omega_{n,m}^2 \left(\frac{R}{\mu_{n,m}}\right)^2 - D\left(\frac{\mu_{n,m}}{R}\right)^2. \tag{15}$$

This is the tension which would produce the expected theoretical value $\omega_{n,m}$ for the frequency of the (n, m) mode. An example (based on the same sound analyzed in the preceding figures) of the resulting T_0 estimate is shown in Fig. 5 for the first 10 modes. As expected, at least for the lowest modes the $T_{0_{n,m}}$ values computed from Eq. (15) are reasonably constant with respect to the mode index, therefore T_0 is estimated to be the average of these values.

In order to estimate values for the dissipation coefficients d_1 and d_3, the decay times t_e for a set of extracted partials have been computed through a Least Squares fitting procedure on the partials amplitudes envelopes. From Eq. (5), one can see that the decay times $t_e(\omega_{n,m})$ decrease with the square of the frequency. More precisely, the following approximate relation holds:

$$t_e(\omega_{n,m}) \simeq \frac{2}{d_1 + d_3 \cdot K \cdot \omega_{n,m}^2}, \tag{16}$$

where $K = \left(\frac{\mu_{n,m}}{R\omega_{0,1}}\right)^2$. Through this fitting procedure the dissipation coefficients d_1 and d_3 were determined. An example of estimated decay time values and the corresponding fitting curve are shown in Figure 6. It can be noticed that t_e values for the lowest modes of vibration are largely overestimated by the damping model. This phenomenon occurs because the model described by Eq. (16) does not include the effect of the air load, which damps strongly the lowest modes. On the other hand for frequencies at 600 Hz or more, the behavior of decay times is more in accordance with theory, as expected. Therefore d_1 and d_3 were determined using partial frequencies above 600 Hz only, while the dissipation coefficients of the lowest modes were manually set in order to cope with the non-ideal behaviour induced by air loading.

Finally analysis of the recorded rototom sounds was performed in order to investigate the effects of tension modulation. Figure 7 shows an example of sound spectra extracted from two frames of the same recording ('strong' level), the first taken close to the impact instant and the second taken after a few tenths of second. The expected effects of membrane nonlinearity can be clearly noticed through comparison of the two spectra: partial frequencies glide in time, with the glide becoming more and more noticeable as the impact velocity increases. In general the glides are concentrated in the first $200 - 300$ ms of the sound.

[1] Note that the computed T_0 value does not necessarily coincide with the real surface tension, since the surface density σ was not measured and instead tabulated values were used.

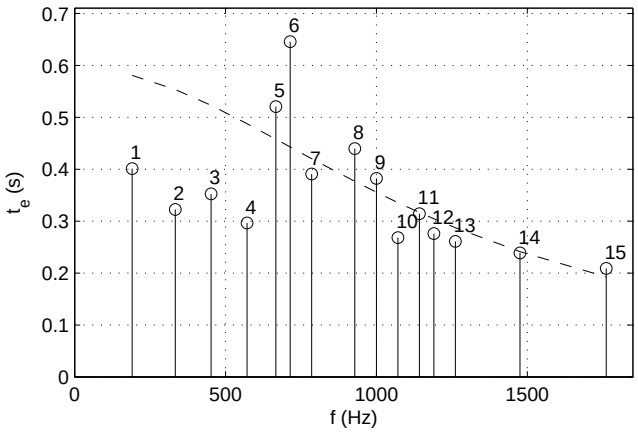

Figure 6: *Estimation of decay times $t_e(\omega_{n,m})$ and LS fitting of the dissipation curve (16).*

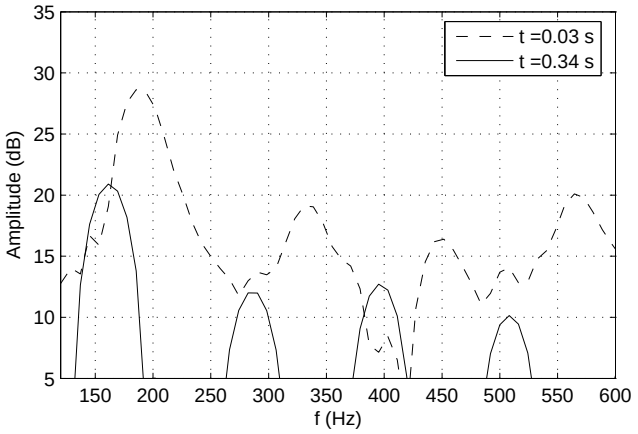

Figure 7: *Effects of tension modulation for high impact velocities: glides of partial frequencies can be clearly noticed by comparing the FFT of a frame close to the attack, and that of a frame a few tenths of second later.*

3.3. Resynthesis

Figure 8(a) shows the spectrogram of a recorded rototom sound, while Fig. 8(b) show the spectrogram of the corresponding resynthesis. It can be noticed that glides in the frequencies of partials are realistically simulated by the numerical model, and resemble closely those observed in the real membrane. Moreover, as a consequence of the analysis procedure outlined in the previous section, the frequencies and the decay times of the modes are accurately simulated in the resynthesis. On the other hand, several distinguishing features of the recorded sound can be noticed in Fig. 8(a). In particular, mode doublets can be observed, which are due to non perfect tuning of the membrane (non constant surface tension). Moreover, a richer spectral content at higher frequencies and at the attack can be noticed. In fact informal listening tests reveal that the simulated impact is qualitatively different from the recorded one, which hints at the limitations of the impact model currently employed.

4. CONCLUSIONS

In this paper, the properties of a recently proposed physical models for sound synthesis of nonlinear circular membranes were investigated. It was shown that tension modulation effects in a struck circular membrane can be simulated by a modal sound synthesis model, by including a nonlinear term that computes the time-varying tension as a function of the membrane displacement.

Comparisons between recorded membrane sounds and numerical simulations show that the model captures the most relevant effect of tension modulation, i.e. variations of frequencies of the membrane modes. Although the focus of the paper is not about exact resynthesis of sounds recorded from real membranes, it has been shown that proper choices of the geometrical and physical parameters of the membrane model result in sound spectra that resemble closely those observed in real circular membranes.

5. REFERENCES

[1] J. O. Smith III, "Virtual acoustic musical instruments: Review and update," *J. New Music Res.*, vol. 33, no. 3, pp. 283–304, Autumn 2004.

[2] V. Välimäki, J. Pakarinen, C. Erkut, and M. Karjalainen, "Discrete-time modelling of musical instruments," *Rep. Prog. Phys.*, vol. 69, no. 1, pp. 1–78, 2006.

[3] S. A. van Duyne and J. O. Smith III, "The 2-D Digital Waveguide Mesh," in *Proc. IEEE Workshop on Applications of Sig. Process. to Audio and Acoustics (WASPAA'93)*, New Paltz (NY), Oct. 1993, pp. 177–180.

[4] F. Fontana and D. Rocchesso, "Signal-Theoretic Characterization of Waveguide Mesh Geometries for Models of Two-Dimensional Wave Propagation in Elastic Media," *IEEE Trans. Speech Audio Process.*, vol. 9, no. 2, pp. 152–161, Feb. 2001.

[5] L. Savioja and V. Välimäki, "Interpolated rectangular 3-d digital waveguide mesh algorithms with frequency warping," *IEEE Trans. Speech Audio Process.*, vol. 11, no. 6, pp. 783–790, Nov. 2003.

[6] M. van Walstijn and K. Kowalczyk, "On the numerical solution of the 2d wave equation with compact fdtd schemes," in *Proc. COST-G6 Conf. Digital Audio Effects (DAFx-08)*, Helsinki, Sep. 2008, pp. 205–212.

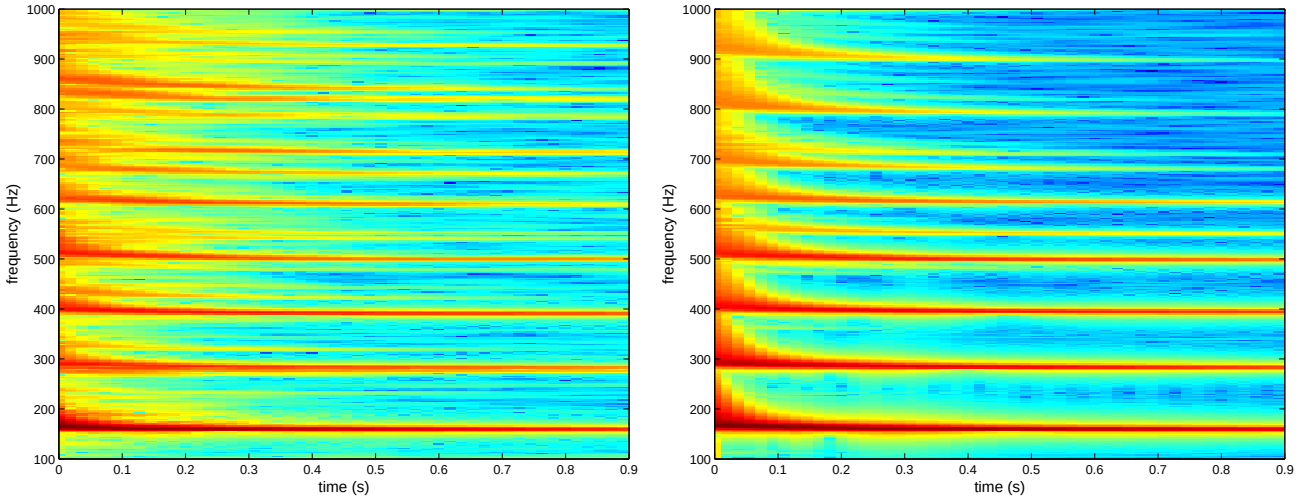

(a) (b)

Figure 8: *Resynthesis of rototom sounds: (a) real rototom STFT; (b) synthetized rototom STFT.*

[7] J.-M. Adrien, "The missing link: Modal synthesis," in *Representations of Musical Signals*, G. De Poli, A. Piccialli, and C. Roads, Eds. Cambridge, MA: MIT Press, 1991, pp. 269–297.

[8] P. R. Cook, "Physically informed sonic modeling (phism): Synthesis of percussive sounds," *Computer Music J.*, vol. 21, no. 3, pp. 38–49, 1997.

[9] L. Trautmann and R. Rabenstein, *Digital Sound Synthesis by Physical Modeling Using the Functional Transformation Method*. New York: Kluwer Academic, 2003.

[10] S. Petrausch and R. Rabenstein, "Tension modulated nonlinear 2D models for digital sound synthesis with the functional transformation method," in *Proc. European Sig. Process. Conf. (EUSIPCO2005)*, Antalya, Turkey, Sep. 2005.

[11] T. Tolonen, V. Välimäki, and M. Karjalainen, "Modeling of tension modulation nonlinearity in plucked strings," *IEEE Trans. Speech Audio Process.*, vol. 8, no. 3, pp. 300–310, May 2004.

[12] S. Bilbao, "Modal type synthesis techniques for nonlinear strings with an energy conservation property," in *Proc. COST-G6 Conf. Digital Audio Effects (DAFx-04)*, Naples, Oct. 2004, pp. 119–124.

[13] R. Rabenstein and L. Trautmann, "Digital sound synthesis of string instruments with the functional transformation method," *Signal Processing*, vol. 83, no. 8, pp. 1673–1688, Aug. 2003.

[14] J. S. Rao, *Dynamics of plates*. New York: CRC Press, 1998.

[15] F. Avanzini and R. Marogna, "A block-based physical modeling approach to the sound synthesis of drums," *IEEE Trans. Audio Speech Lang. Process.*, 2009, *Submitted for publication*.

[16] T. D. Rossing and N. H. Fletcher, *Principles of Vibration and Sound*. New York: Springer-Verlag, 1995.

[17] N. H. Fletcher and T. D. Rossing, *The physics of musical instruments*. New York: Springer-Verlag, 1991.

[18] K. H. Hunt and F. R. E. Crossley, "Coefficient of restitution interpreted as damping in vibroimpact," *ASME J. Applied Mech.*, vol. 42, pp. 440–445, June 1975.

[19] F. Avanzini, M. Rath, D. Rocchesso, and L. Ottaviani, "Low-level sound models: resonators, interactions, surface textures," in *The Sounding Object*, D. Rocchesso and F. Fontana, Eds. Firenze: Mondo Estremo, 2003, pp. 137–172.

[20] F. Fontana and F. Avanzini, "Computation of delay-free nonlinear digital filter networks. Application to chaotic circuits and intracellular signal transduction," *IEEE Trans. Sig. Process.*, vol. 56, no. 10, pp. 4703–4715, Oct. 2008.

[21] F. Fontana and D. Rocchesso, "Physical modeling of membranes for percussion instruments," *Acta Acustica united with Acustica*, vol. 84, no. 3, pp. 529–542, May 1998.